Gas Transfer of an Implatable Artificial Lung

Kyung-Hwa Kim[1], Jong-Beum Choi[2], Gi-Beum Kim[*3]

[1,2,3]Chonbuk National University Medical Schools, Chonbuk National University,
Duckjin-dong 1ga, Duckjin-gu, Jeonju, South Korea
[1]tcskim@jbnu.ac.kr; [2]jobchoi@jbnu.ac.kr; [*3]kgb70@jbnu.ac.kr

***Abstract*-The water flow characteristics in the implantable artificial lung (IAL) were evaluated by in vitro experiments. The 50-fiber modules were of different lengths but contained well-spaced fibers; and the 300-fiber module had a volume fraction of 0.9. A lower number of tired hollow fibers produce a higher water-side film coefficient of oxygen transfer at a constant velocity of water-side flow. The area of the water flow decreases with increasing hollow fiber packing density, thus if water is induced to flow uniformly in the IAL module, the oxygen transfer rate should monotonously increase with the packing density. The water flow in the IAL is not uniform and depends on the hollow fiber packing density. The stagnation of the water flow occurs in the bundle of the hollow fibers at the water inlet.**

Keywords- Implantable Artificial Lung; Hollow Fiber Membranes; Mass Transfer Coefficient; Gas Diffusion

I. INTRODUCTION

Acute respiratory distress syndrome (ARDS) refers to reversible, noncardiogenic pulmonary edema arising from a variety of different insults to the lung tissue. The disease affects approximately 150,000 people per year in the United States [1] and its treatment requires respiratory support using conventional therapies of mechanical ventilation, and/or extracorporeal membrane oxygenation (ECMO) for patients with severe ARDS. The positive airway pressures and volume excursions associated with mechanical ventilation can result in further damage to lung tissue, including barotrauma (high airway pressures), volutrauma (lung distension) and parenchyma damage from the toxic levels of oxygen required for effective mechanical ventilation [2]. The alternative to ECMO is complicated and expensive, requiring extensive blood/biomaterial contact in extracorporeal circuits, systemic anticoagulation, and labor-intensive patient monitoring. Due to these complications, the mortality rate of ARDS patients remains high, exceeding 50% in adults [3-6].

Intravascular oxygenation represents an attractive, alternative support modality for patients with ARDS. The concept of intravascular oxygenation as an alternative ARDS therapy originated with Mortensen [7], who developed an intravenous oxygenator (IVOX) consisting of a bundle of crimped hollow fiber positioned in the vena cava. In phase I clinical trials, the IVOX provided an average of 28% of basal gas exchange requirements for patients with severe ARDS [8-14]. The clinical study, however, concluded that more gas exchange was needed for intravascular oxygenation to be clinically effective in ARDS treatment. We are developing an intravenous membrane oxygenator (IMO) with a design goal of 50% of basal oxygen and carbon dioxide exchange requirements for end-stage ARDS patients. Like the IVOX, the IMO consists of a bundle of manifolded hollow fiber, and is intended for intravenous placement within the superior and inferior vena cava. The target level of gas exchange in the IVOX, and consequently, the IMO, incorporates a polyurethane balloon concentric with the fiber bundle, which rhythmically inflates and deflates to provide active blood mixing, and thus enhances gas exchange. Our current efforts focus on device improvements intended to provide the target levels of gas exchange, given the constraints imposed by intravenous placement on fiber bundle size and hence fiber area for gas exchange. Although critical care techniques have been improved, the high mortality of severe ARDS has not significantly changed [10-15]. In an implantable artificial lung (IAL), the greater part of the oxygen transfer resistance is located in the blood-side laminar film [16], and various methods have been attempted to make the laminar film thin and improve the oxygen transfer rate [17, 18].

In the present study, the water flow characteristics in the IAL were evaluated by in vitro experiments. The effect of hollow fiber packing fraction on water flow condition was evaluated to produce effective constant of water with the hollow fibers. Oxygen transfer rates were evaluated, and the optimum hollow fiber packing fraction was determined at an outside diameter of hollow fibers of 380 μm.

II. THEORYT

The Reynolds number (N_{Re} =Lv/υ) characterizes the flow regime and is the ratio of inertial force to viscous force. The Schmidt number (N_{Sc}=υ/D), analogous to the Prandtl number in heat transfer, characterizes the fluid properties and is the ratio of momentum transport to diffusive transport. The Peclet number (N_{Pe}=Lv/D), which is the product of N_{Re}, characterizes the relative importance of convective and diffusive processes and is the ratio of bulk mass transport to diffusive mass transport. The Sherwood number (N_{Sh}=KL/D), also known as the mass transfer Nusselt number, likewise characterizes the relative importance of convective and diffusive transport; it is the ratio of total transport to diffusive transport. The mass transfer Stanton number (N_{St}=K/v) is proportional to the ratio of the actual mass flux to the mass flux capacity of the flow, i.e. the amount of mass potentially transferable per unit time and cross-sectional area.

DOI: 10.5963/BER0303002

In the expressions of these numbers, L is the characteristic length, v denotes velocity, D denotes diffusivity, υ denotes kinematic viscosity and K denotes mass transfer rate. The overall mass transfer coefficient K is calculated by the following equation.

$$K = -\frac{Q_L}{AH'}\ln[1 - H'(\frac{[O_2]_{in} - [O_2]_{out}}{[O_2{}^*]_{in} - [O_2]_{out}})] \tag{1}$$

where Q_L is the liquid flow rate, A is the interfacial area, $[O_2]_{in}$ and $[O_2]_{out}$ are the inlet and outlet oxygen concentration in the liquid, respectively, and $[O^*{}_2]_{in}$ is the liquid concentration in equilibrium with the inlet gas concentration. The dimensionless group H' is defined as

$$H' \equiv (1 - \frac{Q_L}{Q_G H}) \tag{2}$$

where Q_G is the gas flow rate, and H is the equilibrium ratio of gas concentration to liquid concentration. In the experiments, $Q_L H$ was usually much greater than Q_L, so H' was essentially equal to one. For oxygen removal, the gas stream was essentially free of oxygen, so $[O^*{}_2]_{in}$ was zero, Eq. (1) is then simplified to

$$K = \frac{Q_L}{A}\ln(\frac{[O_2]_{in}}{[O_2]_{out}}) \tag{3}$$

Thes mass transfer coefficients reported in the following section [19, 20].

III. EXPERIMENTAL SETUP

Fig. 1 shows the schematic diagram of the tested IAL device. The IAL tested was prepared with the number of tied hollow fibers in a bundle varying from 50 to 300, as shown in this figure. The distance between the hollow fibers in a bundle was constant for any number of tied hollow fibers. The hollow fiber membrane was made of microporous polypropylene with an outer diameter of 380 μm, thickness of 50 μm and length of 120 cm (Oxyphane, Enka, Germany).

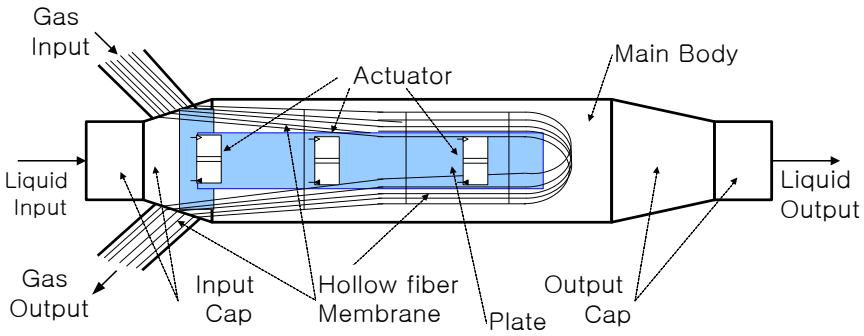

Fig. 1 Detail of the test module

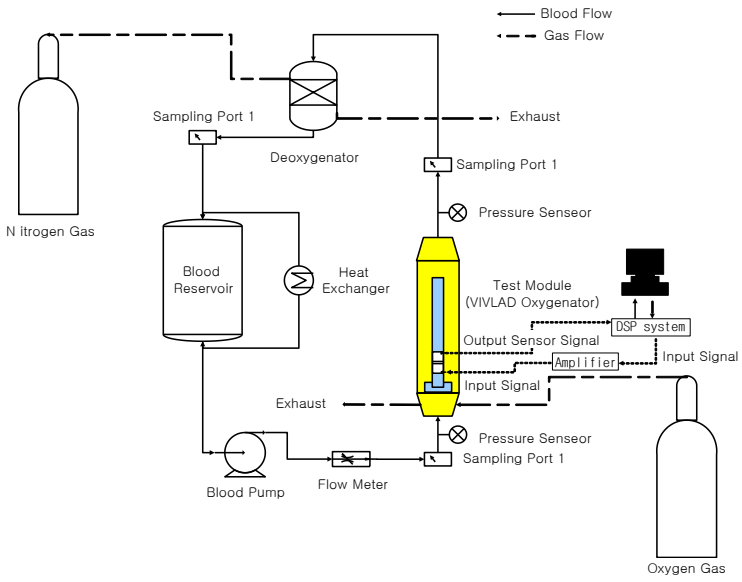

Fig. 2 In vitro bench test system used for the oxygen transfer and of the test modules

DOI: 10.5963/BER0303002

Fig. 2 shows a schematic diagram of the experimental circuit for the measurement of oxygen transfer rate. Deoxygenated water was induced to flow in flow rates ranging from 2 to 6 L/min. The temperature was maintained at 37 ℃ throughout the apparatus. Water was sampled at the inlet and outlet of the IAL module and the partial pressure of oxygen was measured with a DO meter (Model 58, Yellow Springs Instrument, USA). The input and output pressure were measured with a mercury manometer (Model M-1000 W/M, Dwyer Instrument, Inc., USA). Each circuit contained a pump, an oxygenator, appropriate polyvinylchloride tubing, and connectors with stopcocks for water sampling. The oxygenator was placed on the outflow side of the roller pump, the polyvinylchloride tubing loop, and a polyvinylchloride reservoir with a sampling port was attached. A Cobe Cardiovascular system pump (Cobe Cardiovascular, Inc., Arvada, Co. USA) was used for the roller pump The water flow was fixed at 1-6 L/min during the test and the gas flow was also fixed at 1-6 L/min (V/Q ratio = 1). The water flow was monitored using an ultrasonic flow meter (Transonic System T108, Ithaca, NY). In order to maintain a temperature of 37±2 ℃, two reservoirs were connected to the heat exchanger, and a water reservoir was placed between these water reservoirs for one to six hours. Samples were taken from the inlet and outlet sampling ports. The pumps were driven for 6 h at a water volume flow rate ranging from 1 to 6 L/min. The water volume flow rates were controlled by adjusting the resistance attached to the outflow tubing and the rotational speed of the pump. The water volume flow rate was monitored with an electromagnetic flow-meter (MFV-1100, 1200, and 2100, Nihon Koden, Tokyo, Japan).

IV. RESULTS AND DISCUSSION

The idea that mass transfer in the water controls decreation gains powerful support from the results in Fig. 3. In this figure, the logarithm of the mass transfer coefficient (K_c), plotted as a Sherwood number, varies with the logarithm of water velocity per modules length, plotted as a modified Peclet number. The 50-fiber modules were of different lengths but contained well-spaced fibers; the 300-fiber module had a volume fraction of 0.9. The values of K_c for these modules of different geometries all fall along this line. This occurs even though the volume fraction of fibers in the module varies from 1 to 9%. Of course, the flow within the fiber is unaltered by events in the fiber wall or outside the fibers, so K_c is similar in all modules. These results imply that the key to oxygen mass transfer is the diffusion in the liquid. For other solutes, the results may not be as simple. This is especially true when the mass transfer is accelerated by chemical reactions in the liquid. Mass transfer in the liquid apparently also controls ox ygen removal when the water flows outside of but parallel to the follow fibers. As in Fig. 3, the mass transfer coefficient is incorporated in a Sherwood number and plotted versus liquid velocity per module length written as a modified Peclet number. The closed-packed 300-fiber module shows mass transfer independent of flow and over 10 times slower than that in the 50-fiber module. Velocity is reported as a Reynolds number. The characteristic length in the Reynolds number is not the internal diameter of the hollow fiber, but an equivalent diameter (d_e) defined as

$$d_e = [\frac{4(\text{Cross-sectional area})}{\text{Wetted perimeter}}].$$

This quantity is often effective for mass transfer correlations. However, when the fibers are closely packed, the mass transfer coefficient becomes independent of flow, as shown in Fig. 4. Under many circumstances, this would be interpreted as evidence that the membrane resistance has become important. In this case, we are not so sure. The membrane resistance almost certainly is not important for less densely packed fibers, so it seems strange that there is through the closely packed fibers, and that the mass transfer is controlled by diffusion through nearly stagnant liquid trapped between the fibers, not by the membrane.

Fig. 5 shows the dependence of water-side film coefficient of oxygen transfer <K> of the water flow in the IAL at varying number of tied hollow fibers. The water-side film coefficient of oxygen transfer increased with the linear velocity of the water flow. A lower number of tired hollow fibers produce a higher water-side film coefficient of oxygen transfer at a constant velocity of water-side flow. These results indicate that the packing of hollow fiber strongly affects the oxygen transfer rate. This figure showed log-log plot of <K> vs. N_{Re} for the experiment for the IAL at varying number of tied hollow fibers. Least-squares fits yield the following equations:

$$\log\langle K\rangle = \log(1.04) + 1.32 \log N_{Re} \text{ (No. of fibers } 50);$$

$$\log\langle K\rangle = \log(1.27) + 1.30 \log N_{Re} \text{ (No. of fibers } 100);$$

$$\log\langle K\rangle = \log(1.91) + 1.25 \log N_{Re} \text{ (No. of fibers } 150);$$

$$\log\langle K\rangle = \log(3.28) + 1.25 \log N_{Re} \text{ (No. of fibers } 200);$$

$$\log\langle K\rangle = \log(3.66) + 0.97 \log N_{Re} \text{ (No. of fibers } 250);$$

$$\log\langle K\rangle = \log(13.77) + 1.15 \log N_{Re} \text{ (No. of fibers } 300).$$

These values for the slope and vertical position were used in equation $\langle K\rangle = \alpha N_{Re}^{\beta}$ to predict oxygen transfer rates in water for the IAL at varying number of tied hollow fibers.

DOI: 10.5963/BER0303002

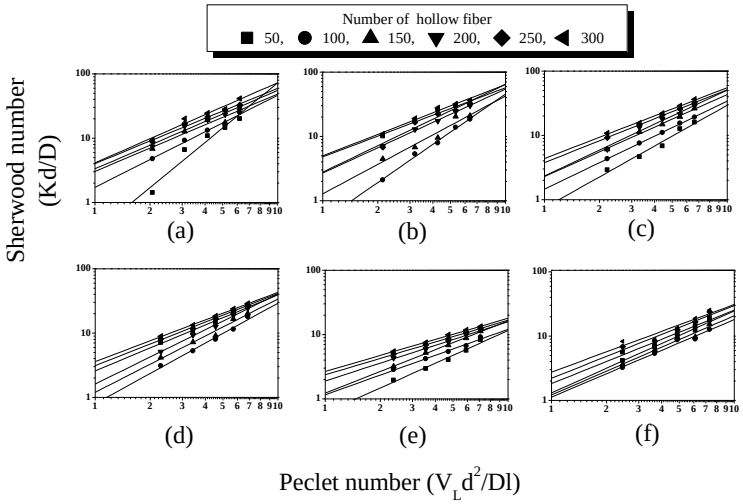

Fig. 3 Mass transfer for water flowing through well-spaced fibers: (a) Gas flow rate 1 lpm, (b) Gas flow rate 2 lpm, (c) Gas flow rate 3 lpm, (d) Gas flow rate 4 lpm, (e) Gas flow rate 5 lpm, (f) Gas flow rate 6 lpm

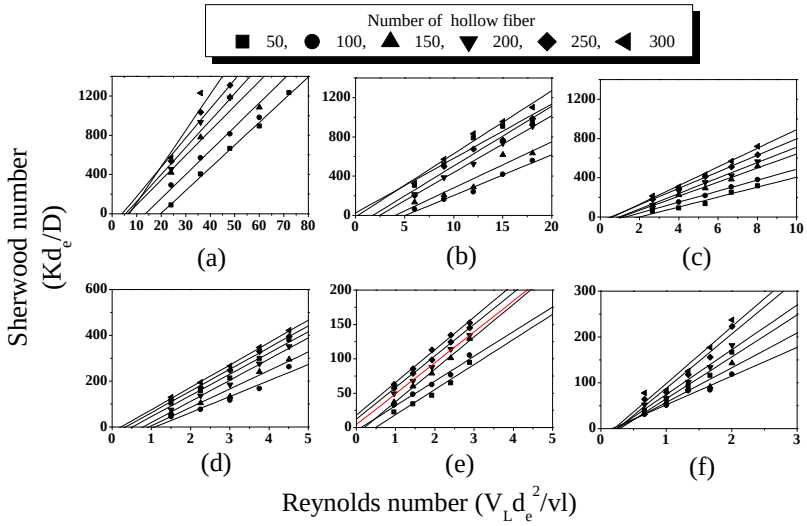

Fig. 4 Mass transfer for water flowing outside and parallel to the hollow fibers: (a)50 fiber, (b) 100-fiber, (c) 150-fiber, (d) 200-fiber, (e) 250-fiber, (f) 300-fiber

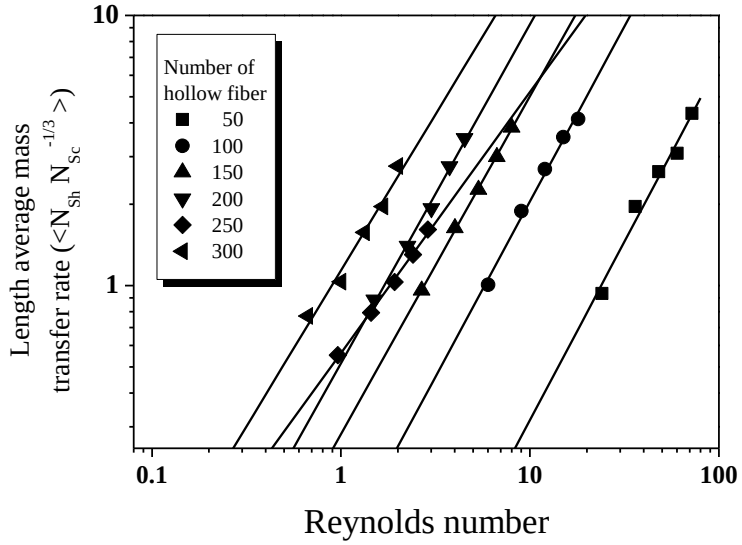

Fig. 5 Relationship between Reynolds number and length average transfer rate at varying the number of tied hollow fibers

Fig. 6 shows the dependence of the oxygen transfer rate of oxygen using water on the hollow fiber packing density of the IAL. The area of the water flow decreases with increasing hollow fiber packing density, thus if water is induced to flow

DOI: 10.5963/BER0303002

uniformally in the IAL module, the oxygen transfer rate should monotonously increase with the packing density. This demonstrates that the water flow is not uniform and different at each packing density.

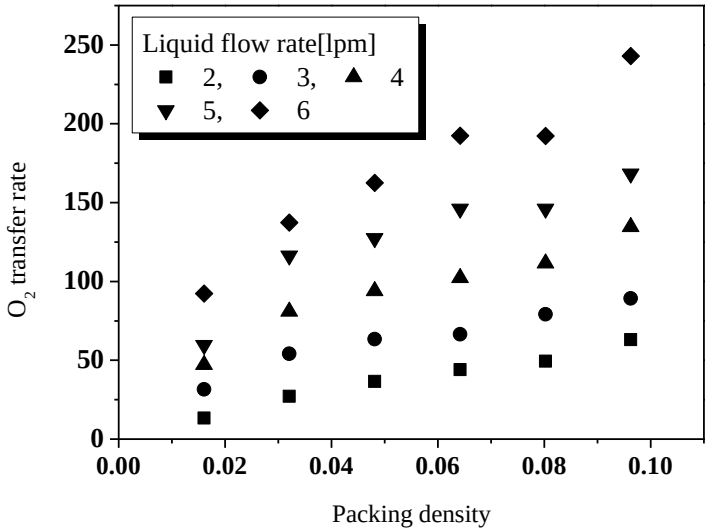

Fig. 6 Dependence of oxygen transfer rate at various numbers of tied hollow fibers

V. CONCLUSIONS

The results reported in this paper strongly indicate that the performance of microporous hollow-fiber is almost always controlled by the mass transfer in the liquid phase. The data in Figs. 3 and 4 are consistent with this conclusion. The mass transfer coefficient itself is reported as a Sherwood number N_{Sh}. The variations in water velocity and module length are reported as a Reynolds number N_{Re} or a modified Peclet number N_{Pe}. Note that the kinematic viscosity v and the diffusion coefficient D have not been varied in our experiments. For parallel flow outside of hollow fibers, the obtained results do not agree with scattered previous correlations for this unbaffled laminar flow. The obvious answer is some type of secondary flow. When we consulted heat transfer experts, they all volunteered this rationalization. However, these same experts could not suggest specific references that support this idea. Oxygen transfer rate of the IAL increased with the increase in the number of tied hollow fibers due to more effective water contact with the membrane. The water flow in the IAL was not uniform and depended on hollow fiber packing density. The stagnation of the water flow occurred in the bundle of the hollow fibers at the water inlet.

ACKNOWLEDGMENT

This work was supported by National Research Foundation of Korea Grant funded by the Korean Government (Ministry of Education, Science and Technology (NRF–2010–359–D00036) and the fund of Chonbuk National University Hospital Research Institute of Clinical Medicine.

REFERENCES

[1] F. L. Fazzalari, R. H. Bartlett, M. R. Bonnell, and J. P. Montoya, “An intrapleural lung prosthesis: Rationale, design, and testing,” *Artifi. Organs*, vol. 18, pp. 801-805, Nov. 1994.

[2] S. E. Weinberger, “Principles of Pulmonary Medicine,” Philadelphia, Saunders, 1992.

[3] L. Gattinoni, A. Agostoni, A. Pesenti, A. Pelizzola, G. P. Rossi, M. Langer, S. Vesconi, L. Uziel, U. Fox, F. Longoni, T. Kolobow, and G. Damia, “Treatment of acute respiratory failure with low-frequency positive-pressure ventilation and extracorporeal removal of CO2,” *Lancet*, vol. 2, pp. 292-294, Aug. 1980.

[4] A. Pesenti, L. Gattinoni, T. Kobolow, and G. Damia, “Extracorporeal circulation in adult respiratory failure,” *ASAIO Trans*, vol. 34, pp. 43-47, Jan-Mar. 1988.

[5] M. T. Snider, D. B. Campbell, W. A. Kofke, K. M. High, G. B. Russell, M. F. Keamy, and D. R. Williams, “Venovenous perfusion of adults and children with severe acute respiratory distress syndrome. The Pennsylvania State University experience from 1982-1987,” *ASAIO Trans*, vol. 34, pp. 1014-1020, Oct-Dec. 1988.

[6] S. Ichiba and R. H. Bartlett, “Current status of extracorporeal membrane oxygenation for severe respiratory failure,” *Artifi. Organs*, vol. 20, pp. 120-123, Feb. 1996.

[7] J. D. Mortensen, “Intravascular oxygenator: a new alternative method for augmenting blood gas transfer in patients with acute respiratory failure,” *Artifi. Organs*, vol. 16, pp. 75-82, Feb. 1992.

[8] S. A. Conrad, A. Bagley, B. Bagley, and R. N. Schaap, “Major findings from the clinical trials of the intravascular oxygenator,” *Artifi. Organs*, vol. 18, pp. 846-863, Nov. 1994.

DOI: 10.5963/BER0303002

[9] T. T. Nguyen, J. B. Zwischenberger, W. Tao, D. L. Traber, D. N. Herndon, C. C. Duncan, P. Bush, and A. Bidani, "Significant enhancement of carbon dioxide removal by a new prototype IVOX," *ASAIO J.*, vol. 39, pp. M719-M724, July-Sep. 1994.

[10] G. B. Kim, C. U. Hung, and T. G. Kwon, "Design of the Intravenous Oxygenator," *J. Artifi. Organs*, vol. 9, pp. 34-41, Mar. 2006.

[11] G. B. Kim, C. U. Hong, S. J. Kim, J. S. Kim, M. H. Kim, and H. S. Kang, "Development of a hollow fiber membrane module for using implantable artificial lung," *J. Mem. Sci.*, vol. 326, pp. 130-136, Jan. 2009.

[12] C. U. Hong, J. M. Kim, M. H. Kim, S. J. Kim, H S. Kang, J. S. Kim, and G. B. Kim, "Gas Transfer and Hemolysis in an Intravascular Lung Assist Device Using a PZT Actuator," *Int. J. Precis. Eng. Manuf.*, vol. 10, pp. 67-73, Jan. 2009.

[13] G. B. Kim, C. U. Hong, J. S. Kim, M. H. Kim and H. S. Kang, "Improvement of gas transfer by hemosome," *Int. J. Artif. Organs*, vol. 33, pp. 171-178, Apr. 2010.

[14] S. J. Kim, K. H. Kim, S. J. Kim, H. S. Kang, J. S. Kim, M. H. Kim, J. K. Jo, J. B. Choi, Y. S. Yang, and G. B. Kim, "Effectiveness of antioxidant and membrane oxygenator in acute respiratory distress syndrome by endotoxin," *Korean J. Chem. Eng.*, vol. 29, pp. 1597-1603, Nov. 2012.

[15] M. A. Woodhead, "Management of pneumonia," *Respir. Med.*, vol. 86, pp. 459-469, Nov. 1992.

[16] S. N. Vaslef, L. F. Mockros, R. W. Anderson, and R. J. Leonard, "Use of a mathematical model to predict oxygen transfer rates in hollow fiber membrane oxygenators," *ASAIO J.*, vol. 40, pp. 990-996, Oct.-Dec. 1994.

[17] H. M. Weissman and L. F. Mockros, "Gas transfer to blood flowing in coiled circular tubes," *J. Eng. Mech. Div. ASCE.*, vol. 94, pp. 857-872, 1968.

[18] K. Tanishita, P. D. Richardson and P. M. Galletti, "Tightly wound coils of microporous tubing: progress with secondary-flow blood oxygenator design," *Trans. Amer. Soc. Artif. Int. Organs*, vol. 21, pp. 216-222, 1975.

DOI: 10.5963/BER0303002